RADIOMETRIC CALIBRATION OF A NOVEL FIELD IMAGING SPECTROMETER SYSTEM (FISS)

Changping Huang[a], Lifu Zhang*[a], Junyong Fang[a], Jinnian Wang[a], Qingxi Tong[a]

[a] The State Key Laboratory of Remote Sensing Sciences, Institute of Remote sensing Applications, CAS
20A Datun Road, Chaoyang District, Beijing 100101, P. R. China
E-Mails: hcp2qq@163.com (C.-P.H., Graduate student, Tel: +86-15101022443); zhanglf@irsa.ac.cn (L.-F.Z., Professor, Tel: +86-13716974736); hrsfang@163.com (J.-Y.F., Associate Professor); jwang@irsa.ac.cn (J.-N.W., Professor); tqxi@263.net (Q.-X.T., Professor);

KEY WORDS: Radiometric Calibration, Pixel Uniformity, Radiometric Linearity, System Noise, Field Imaging Spectrometer System (FISS)

ABSTRACT: Based on our previous work, this paper further investigated radiometric properties of a novel field imaging spectrometer system (FISS), the first imaging sensor aimed specifically at field imaging spectrometry in China. Using a well-calibrated integrating sphere and a diffuse reflectance standard, two independent laboratory and field experiments were carefully designed to jointly calibrate the FISS radiometrically. Among all the radiometric properties of FISS, four critical ones were chosen and thoroughly analyzed, including radiometric temporal stability, pixel uniformity, response linearity and system noise. Calibration results show that (i) the 2-dimensional cooled array CCD in FISS undergoes an average pixel non-uniformity of less than 7% and temporal stability of ~2.5% both evaluated by the coefficient of variation; (ii) FISS has a good radiometric linearity between input radiance and output DN values with the calibration accuracy of $R^2 \geq 0.99$ and NRMSE (normalized root-mean-square-error) ~0.01 for each spectral channel; and (iii) the FISS system performs in a high signal to noise ratio level due to the employment of a semiconductor refrigeration technology in the array CCD camera, which produces a low dark offset of ~5DN if the cooled temperature lower than 20℃. Additionally, to meet the requirement of precision quantitative applications, FISS was relative radiometrically corrected by histogram equalization and the spectral smile problem of FISS was discussed as well. In contrast with our earlier work, this study not only further demonstrates that FISS has achieved high performance, but provides useful guidelines to make good use of it, meanwhile promotes better understanding of FISS-type sensors.

1. INTRODUCTION

Many of traditional space-/airborne and ground-based remote sensors are limited to being purely image-based (e.g., LandSat/Thematic Mapper) or purely spectroscopy-based (e.g., ASD FieldSpec Pro FR) sensors. In contrast, imaging spectrometry—combining the image and spectrum of an object—has aroused growing interest as a novel technique for remote sensing. Such sensors, as the Airborne Visible/Infrared Imaging Spectrometer(Goetz 2009), have successfully been used in specific target detection, precise classification, and quantitative retrieval. Nevertheless, wider use of imaging spectrometry is also limited because ground resolution of only a few meters to several kilometers is typically achieved.

To solve these issues, field imaging spectrometers are especially concerned because of their improved spatial resolution. Many countries—including the United States and Japan—have launched a series of mature field imaging spectrometers(Ye et al. 2008) which have been successfully used in agriculture, food monitoring, vegetation observation, and geological mapping. However, to the best of our knowledge, no such device has been

reported in China. To address this need, we have developed a novel field imaging spectrometer system (FISS) on the basis of the Chinese aviation push-broom imaging spectrometer (PHI)(Zhang et al. 2000).

The FISS is the first imaging sensor aimed specifically at field imaging spectrometry in China. For a scientific instrument, system calibration is the fundamental step before its applications, and FISS is no exception. In our earlier work(Tong et al. 2010; Zhang et al. 2011), it has been primarily introduced and calibrated. FISS measures the incoming radiation in 344 contiguous spectral channels in the 437-902nm wavelength range with the spectral resolution of better than 5nm and images 464 pixels of a line of targets with a nominal instantaneous field of view (IFOV) ~1mrad. Differing from the PHI, the second spatial dimension of FISS is performed by a scan mirror within a certain angle and record rate driven by a stepper motor. Although initial applications by FISS have also been successfully conducted in our institution(Tong et al. 2010), for precision researches and applications, more detailed characterization and calibration for it should be explored.

The objective of this paper is to further investigate radiometric characteristics of FISS in terms of radiometric temporal stability, pixel uniformity, radiometric linearity and system noise. To pursue high-quality images, relative radiometric correction and spectral smile effect of FISS are also specially considered. This study, therefore, matters in better employing the FISS and understanding FISS-type sensors.

2. FISS RADIOMETRIC CALIBRATION METHODS

2.1 Radiometric Calibration Experiments

Two radiometric calibration experiments—including laboratory and field experimental set-ups utilizing artificial and natural light sources respectively— were carefully designed to better calibrate the FISS. Therefore, calibration results from the two experiments can be verified each other.

Laboratory experiment was accomplished in a precise optic laboratory by an integrating sphere and a SVC HR-1024 field portable spectrometer both well calibrated. The HR-1024 spectrometer, located in the same horizontal plane as FISS in front of the integrating sphere, was used to cross-calibrate our FISS. The two sensors, both fully illuminated, simultaneously recorded data under 17 radiance levels by controlling the number of lighting bulbs inner the integrating sphere. Throughout the experiment, FISS kept the same system settings with the integrating time of 30ms, cooled temperature of 10 ℃, and aperture of F/16. In laboratory, dark offset, consisting of dark current noise and read noise, was measured under 100 combinations of the cooled temperature and integrating time by keeping the light entrance slit closed. The cooled temperature changed within the range of -5~40℃ with an interval of 5℃, while the integrating time within the range of 10~100ms with an interval of 10ms.

Field experiment, mainly designed for further evaluating the radiometric stability / uniformity and spectral smile effect of FISS, was conducted in a clear day with a uniform diffuse reflectance standard filling with the field of view (FOV) of FISS. To evaluate radiometric stability, the FieldSpec HandHeld Spectroradiometer (spectral range, 350~1050nm; spectral resolution, ~3.5nm) was used as a standard at the same time every 3 minutes.

2.2 Radiometric Uniformity and Stability

Slight variation in quantum efficiency may occur to FISS pixels as a result of the processing error during CCD fabrication(Garcia et al. 2005). For the sake of these variations in pixels along the spatial axis of the array CCD, even if FISS is uniformly illuminated, it will introduce fixed pattern non-uniformity. To accurately evaluate the pixel uniformity, two images separately obtained by FISS in laboratory and field were adopted. Using the coefficient of variation (CV), the pixel uniformity of detectors along each channel was calculated as formula (1).

$$CV_i = Std_i / Mean_i \quad (1)$$

Where Std_i and $Mean_i$ are the standard deviation and mean value of the 464 pixels at the ith spectral channel respectively. Owing to slight heterogeneity among detectors, FISS must be corrected to accurately extract scene characteristics. In this paper, correction coefficients were derived by histogram equalization(Guo et al. 2005).
The radiometric temporal stability for each pixel, reflecting measurement repeatability during certain working hours, was also determined by the CV method. In this case, the subscript i in Eq. (1) stands for pixel No..

2.3 Radiometric Response Linearity

Radiometric linearity, as the foundation of the absolute radiometric calibration(Zhang et al. 2011), is often used for evaluating the linear relation between input radiance (Le) and output DNs of remote sensors. Based on the following equation (2), FISS radiometric linearity was investigated band by band. And then, the determination coefficient (R^2) and normalized root-mean-square error (NRMSE, defined as Eq. (3)) were applied to assess the goodness of linear fitting models for all the channels.

$$DN = Gain \cdot L_e + Offset \quad (2)$$

$$NRMSE = \frac{\sqrt{\sum_{i=1}^{L}(DN_{m\_i} - DN_{p\_i})^2 / L}}{DN_{\max} - DN_{\min}} \quad (3)$$

In equation (3), L is the number of the radiance levels, DN_{m_i} and DN_{p_i} are measured and predicted DNs of the ith radiance level respectively, $DN_{\max}$ and $DN_{\min}$ are the maximum and minimum values of measured DNs respectively.

2.4 System Noise

No scientific instrument can perform noise-free, nor can the FISS. Various kinds of noise (Ortiz and Oliver 2004)will contaminate the ideal pixel values and result in poor-quality images. Dark current and read noise, incorporated as dark offset, were measured as section 2.1. Shot noise, non-additive noise governed by a Poisson distribution, was investigated by altering radiance levels of the integrating sphere. Fixed pattern noise, caused by pixel non-uniformity, is not dominant noise source for FISS.

3. RESULTS AND DISSCUSSIONS

3.1 Radiometric Uniformity and Stability

Using Eq. (1), FISS radiometric pixel uniformity of each spectral channel was calculated. Figure 1 shows CV values against FISS spectral channels, where figure 1(a) is the results calculated from an integrating sphere image acquired in laboratory with mean uniformity over the 344 channels of CV_{mean}=0.066194 and the corresponding standard deviation CV_{std}=0.017725; figure 1(b) is the results derived from a diffuse reflectance standard image obtained in field with the CV_{mean}=0.068205 and CV_{std}=0.019923. Generally, an array CCD might undergo pixel non-uniformity within a range of 7~15%(Yang et al. 2004), which implies that FISS has achieved acceptable pixel uniformity (CV_{mean} < 7%). If the non-uniformity of calibration facilities such as the integrating sphere and diffuse

reflectance standard considered, FISS will enjoy better pixel uniformity. However, for precision applications, slight variations in detectors may introduce obvious errors. Hence pixel non-uniformity should be corrected. Using histogram equalization method, FISS was relatively corrected for all the spectral channels. Figure 2(b) displays the correction result of figure 2(a), the channel 100 of the laboratory integrating sphere image, and the corresponding relative gain coefficients against column positions are given in figure 2(c), most of them close to unity.

In figure 1(b), significant fluctuations occur particularly in the 239, 240, 241and 242 spectral channels, where the CV values are much higher than others, on the order of 17.1123%, 28.0712%, 22.0444% and 13.2646%, but the same case cannot be seen in figure1(a). These fluctuations may be caused by spectral smile effect due to sharp absorption of Oxygen-A feature (760nm) in the channel 241of FISS. It's proved that very often sensors with two-dimensional detector arrays such as EO-1/Hyperion suffer from spectral smile problem(Ceamanos and Doute 2010), and FISS of the same type is no exception. Spectral smile can be detected by minimum noise fraction (MNF) transformation or band difference technique around Oxygen-A feature. Applying the two methods respectively, clear brightness gradient, indicator of significant smile effect, can be seen from both the first eigenimage of MNF space and the difference image between the channel 242 and 240 in figure 3.

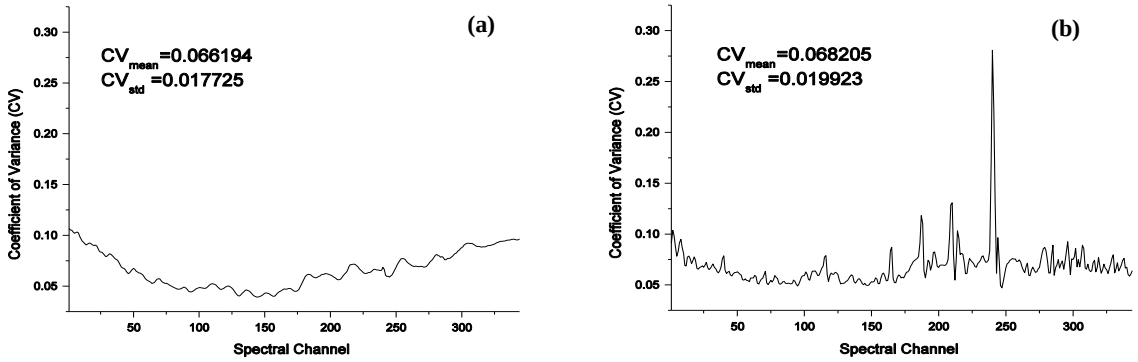

Fig.1 CV values against 344 spectral channels of FISS: (a) laboratory results; (b) field results

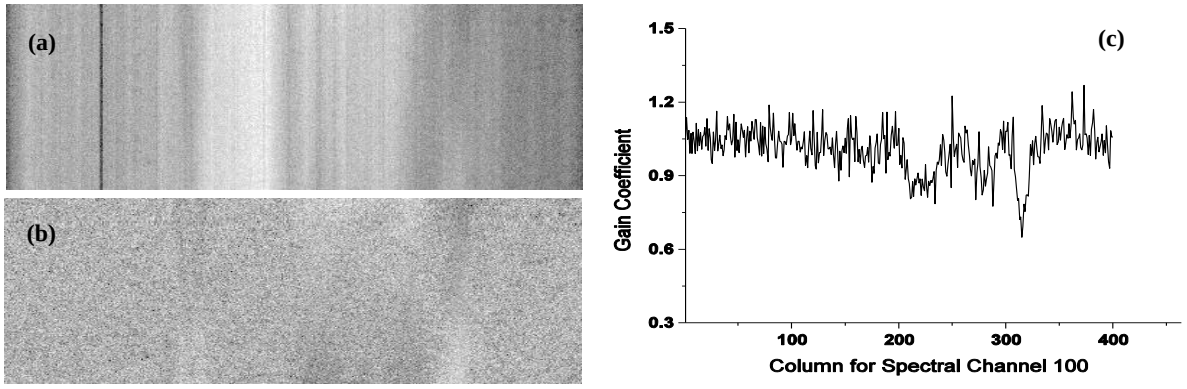

Fig.2 Relative radiometric correction for channel 100 from laboratory integrating sphere image: (a) Original image; (b) Corrected image; (c) Relative gain coefficients against column positions

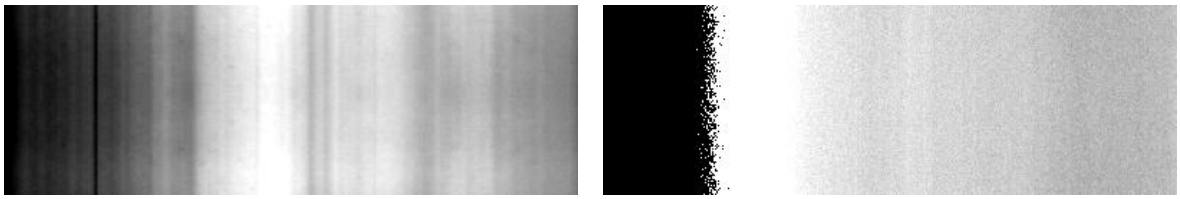

Fig.3 First eigenimage of MNF space (Left) and difference image between the channel 242 and 240 around Oxygen-A feature (Right) showing clear brightness gradient mainly caused by spectral smile effect

Results from figure 3 verify that FISS suffers from smile problem, which is especially acute around the sharp

absorption channel of Oxygen-A feature. Spectral smile will affect the accuracy of quantitative applications, so desmiling techniques for FISS should be investigated in the future.

Based on Eq. (1), radiometric temporal stability for each detector of FISS and FieldSpec HandHeld Spectroradiometer was separately calculated using five data sets obtained every 3 minutes. Results demonstrate the mean CV values of the two instruments are almost identical, about 2.5%, confirming that FISS shares the similar radiometric temporal stability with FieldSpec HandHeld Spectroradiometer that is recognized very stable.

3.2 Radiometric Response Linearity

The radiometric linearity of FISS was investigated spectral channel by channel on the basis of the method mentioned in section 2.3. Figure 4 shows the calibration result of spectral channel 13, where the solid line is "y=x". Figure 5 displays the R^2 (blue curve to left ordinate) and NRMSE (red curve to right ordinate) of all linear fit models against the 344 spectral channels, of which the calibration accuracy of $R^2 \geq 0.99$ and NRMSE is ~0.01 for each channel. From the two figures, we can conclude that FISS is a high linear response system.

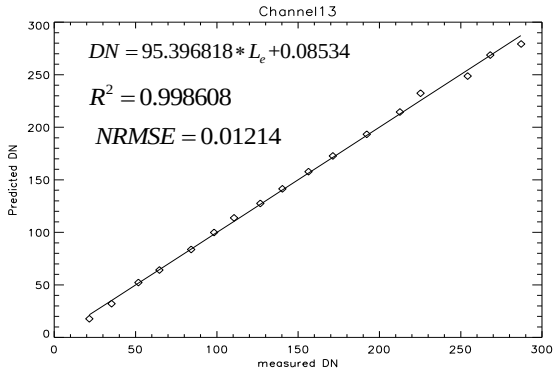

Fig.4 Response linearity of FISS for channel 13

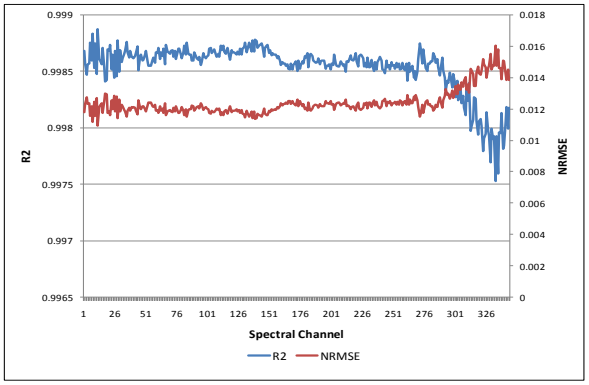

Fig.5 R^2 (Blue) and NRMSE (Red) against 344 spectral channels

3.3 System Noise

Figure 6 plots the mean dark offset variations of the array CCD with the cooled temperature and integration time, which demonstrates that if the cooled temperature lower than 20℃, the dark offset will almost keep invariant of ~5 DN, whereas if higher than 20℃, the dark offset is proportional to the integration time and highly temperature dependent. In actual applications, it's easy for users to control the CCD working temperature below 20℃ because of semiconductor refrigeration technology applied in FISS, assuring acquisitions of high-quality images by FISS

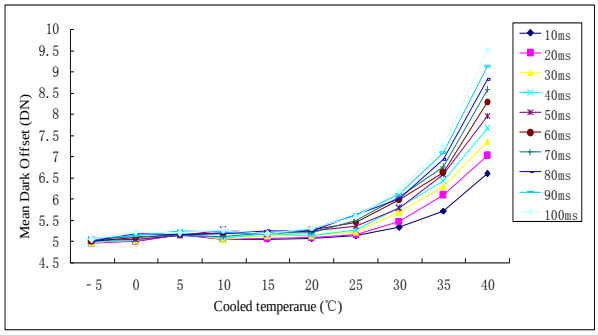

Fig.6 Variations of mean dark offset with temperature and integration time

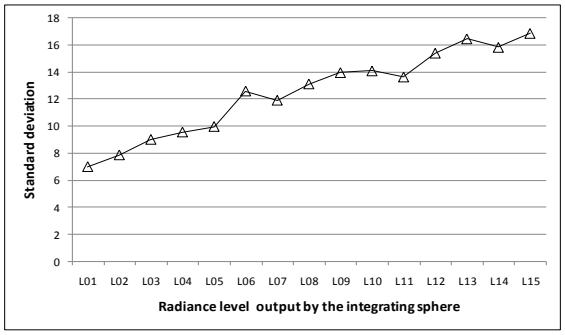

Fig.7 Variations of shot noise with radiance levels

FISS shot noise was simply measured by altering radiance levels of the integrating sphere. Figure 7 shows that shot noise, defined by standard deviation of one chosen pixel (232,150) from the CCD chip, changes over radiance levels (totally 15 levels named from L01 to L15 as the abscissa), which implies that shot noise increases with the

signal intensity input in most cases. Due to pixel non-uniformity as section3.1 described, fixed pattern noise also appears in FISS, but it can be easily estimated and removed using the existing methods(Ortiz and Oliver 2004).

4. CONCLUSIONS AND PROSPECTS

By designing laboratory and field experiments respectively, the newly developed FISS was further radiometrically calibrated on the basis of our previous work. Four critical radiometric properties including radiometric temporal stability, pixel uniformity, response linearity and system noise, were accurately calibrated and analyzed in this paper. This study further demonstrates that China's first field imaging spectrometer has achieved high performance. Besides, by identifying weak and strong points of FISS, users can better employ it and understand FISS-type sensors. No instrument is perfect, and FISS also cannot escape from some problems such as spectral smile effect because of the arrangement of its two-dimensional detector arrays, which will affect the accuracy of its quantitative applications. Therefore, to acquire high quality images by FISS, ongoing efforts must be made.

5. ACKNOWLEDGEMENT

The authors gratefully acknowledge the support of the National Natural Science Foundation of China (Project Number 30772890, 41072248) and the Director's Scholarship of the Institute of Remote Sensing Applications in the Chinese Academy of Sciences (Project Number Y0S01900KB).

6. REFERENCES

Ceamanos, X., & Doute, S. (2010). Spectral smile correction of CRISM/MRO hyperspectral images. *Geoscience and Remote Sensing, IEEE Transactions on, 48*, 3951-3959

Garcia, C., Refaat, T., Farnsworth, G., Abedin, M., & Elsayed-Ali, H. (2005). Characterization of InGaAs linear array for applications to remote sensing. In (p. 57): SPIE, the International Society of Optical Engineering

Goetz, A.F.H. (2009). Three decades of hyperspectral remote sensing of the Earth: A personal view. *Remote Sensing of Environment, 113*, S5-S16

Guo, J., Yu, J., Zeng, Y., Xu, J., Pan, Z., & Hou, M. (2005). Study on the relative radiometric correction of CBERS satellite CCD image. *Science in China Series E: Technological Sciences, 48*, 12-28

Ortiz, A., & Oliver, G. (2004). Radiometric calibration of CCD sensors: Dark current and fixed pattern noise estimation. *2004 Ieee International Conference on Robotics and Automation, Vols 1- 5, Proceedings*, 4730-4735, 5306

Tong, Q., Xue, Y., Wang, J., Zhang, L., Fang, J., Yang, Y., Liu, X., Qi, H., Zheng, L., & Huang, C. (2010). Development and application of the field imaging spectrometer system. *Journal of Remote Sensing, 14*, 409-422

Yang, W., Pan, L., Hong, J., & Qiao, Y. (2004). Radiometric Calibration of Multi-band Polarization CCD Camera. *High Technology Letters, 14*, 11-15

Ye, X., Sakai, K., Okamoto, H., & Garciano, L. (2008). A ground-based hyperspectral imaging system for characterizing vegetation spectral features. *Computers and Electronics in Agriculture, 63*, 13-21

Zhang, B., Wang, X., Liu, J., Zheng, L., & Tong, Q. (2000). Hyperspectral image processing and analysis system (HIPAS) and its applications. *Photogrammetric Engineering and Remote Sensing, 66*, 605-610

Zhang, L., Huang, C., Wu, T., Zhang, F., & Tong, Q. (2011). Laboratory Calibration of a Field Imaging Spectrometer System. *Sensors, 11*, 2408-2425